Preprints of the 21st IFAC World Congress (Virtual)
Berlin, Germany, July 12-17, 2020

Spacecraft INS/CNS/Pulsar integrated Positioning Navigation and Timing

Hamza Benzerrouk *,**Vladimir Nebylov**,**Alexander Nebylov**, **Rene.Jr Landry***

* *Ecole de Technologies Superieure- ETS Montreal,CANADA, Laboratory of Space Technologies, Embedded Systems, Navigation and Avionics LASSENA -, e-mail: hamza.benzerrouk@lassena.etsmtl.ca, St Petersburg State Aerospace Instrumentation-SUAI 2310 Bolshaya Morskaya, St petersburg, Russia 190000,email: nebylov@aanet.ru Hamza Benzerrouk is the corresponding author.*

Abstract: In this paper, robust algorithms of information fusion between Pulsars timing, ranging and positioning with orbital dynamical model of explorer spacecraft is demonstrated with combination to inertial navigation system. Pulsar/CNS integration is considered in this work and was recently investigated using multiple variant of nonlinear filtering approaches, providing an interesting advances and results. However, due to the colored measurement noise from pulsars time of arrival measure, robust nonlinear filter has been derived based on Gauss Quadrature Kalman filters at different degrees. Moreover, because it has been demonstrated that in the during short period of observation, and minimum photons numbers, the noise affecting the X-Ray signal becomes not a Gaussian distribution. An alternative solution to this problem is proposed using multiple quadrature Kalman filters derived in the Gaussian Sum framework. At last, as an experimental validation, the Crab pulsar data were used to demonstrate the efficiency of the novel robust filtering approach against non linearity and also colored non Gaussian measurement noises.

Keywords: Pulsar, CNS, non Gaussian noise, TOA, Quadrature Kalman Filter, Clock drift.

1. INTRODUCTION

Recently, deep space exploration based on autonomous navigation systems has attracted the scientific community for its relevant and multiple challenges. The state of the art in this field has elegantly used CNS (Celestial navigation system)[1] based on horizontal and elevation angle measurement embedded on board spacecraft's navigators. In order to enhance the navigation accuracy, different techniques and measures were developed and investigated. The most famous techniques are Doppler/CNS integrated navigation approaches[2,4,5] being proposed in the last decades, even if at the end, this method was carrying out unsuitable performances for autonomous deep space navigation. In parallel, inertial navigation systems are the widely used integrated sensors for different navigation problems, on Earth, in Space and also considered for deep space exploration, such as Mars exploration, solar systems exploration, and future challenging missions[7,8,11,12].

However, due to the drift of inertial sensors, other corrections over the navigation epochs remains necessary and an ingenious principle was then proposed in the literature and tests on real spacecraft [7,8,14]. This source of correction is called Pulsars, timing sources in the universe, which are rapidly rotating neutron stars that generate pulsed electromagnetic radiation in the X-Ray spectrum. Since their discovery [8], it has been demonstrated that a unique signal delivered by these sources can be detected by X-ray sensors, especially when embedded onboard spacecraft. In addition, by using TOA (Time-of-arrival) after 10 minutes of observation. It is possible to construct TDOA(Time Difference of Arrival) between TOA at the spacecraft and TOA predicted at the SSB (Solar system barycenter), due to what, stellar position of spacecraft can be then estimated accurately[9].

In parallel to this attractive principle and solution, very nice performances are achieved when we consider the measurement noise distribution as a Gaussian, which is not totally true [4,6]. For this purpose, we consider a very short period of observation during what CNS and Pulsar X-Ray TOA measures are affected by non Gaussian noises. To handle that, we first propose an integrated INS/CNS/Pulsar navigation and Timing system. Then, assuming non Gaussianity of the environment, modification of the large family of nonlinear filtering approaches, all Kalman based, is proposed and derived in the Gaussian Sum Framework. Extended Kalman Filter (EKF) , UKF (Unscented Kalman Filter), Cubature Kalman Filter (CKF), and Gauss Hermite Kalman Filters (GHKF)[3,4] are adopted to perform against non-linearity [4]. Thus, they are modified into Gaussian sum filters to perform better against non-Gaussianity. In this paper, CNS based on horizontal and vertical sensor is assumed, delivering elevation angle at short period of times. In parallel, we assume that only one X-ray pulsar from Crab nebula is delivering non Gaussian measurement during very short observation period. In our case, Crab-nebula pulsar was selected as the most accurate timing source among other

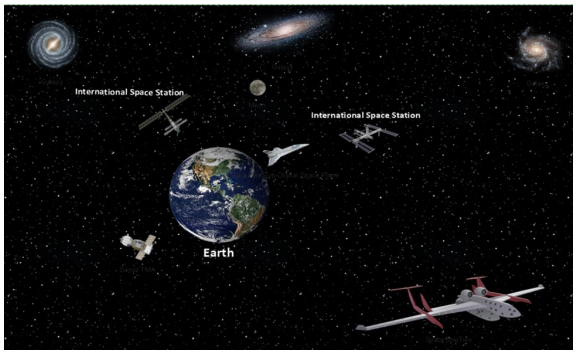

Fig. 1. Artist image of spacecraft navigation in deep space of our solar system

pulsars databases. Furthermore, infinite Millisecond as well as microsecond pulsars in different galaxies could be considered in a future more advanced work for deep space exploration.

2. INERTIAL NAVIGATION EQUATIONS

The basic inertial navigation equations have been derived and implemented following the model [7,8,11,12,13]. In the following, navigation equations are derived as continuous time state space models and discrete time state space model. Both spaces representations present non-linearity degrees.

where VN, VE and VD are the north, east and down velocities in the local tangent plane, with reference to a local geodetic frame often referred to as the navigation frame (n-frame) or north-east-down frame. From which one can integrate Latitude, Longitude and altitude in the navigation frame. In our case, these are celestial coordinates such as described on Fig.3. Below, inertial navigation differential equations:

$$\begin{bmatrix}\dot{V}_N\\ \dot{V}_E\\ \dot{V}_D\end{bmatrix} = \begin{bmatrix}A_N\\ A_E\\ A_D\end{bmatrix} + \begin{bmatrix}0\\ 0\\ g\end{bmatrix} + \begin{bmatrix} -\left(2\omega_s \sin\lambda + \frac{V_E}{R_P+h}\tan\lambda\right)V_E + \frac{V_N V_D}{R_M+h} \\ \left(2\omega_s \sin\lambda + \frac{V_E}{R_P+h}\tan\lambda\right)V_N + \left(2\omega_s \cos\lambda + \frac{V_E}{R_P+h}\right)V_D \\ -\frac{V_N^2}{R_M+h} - \left(2\omega_s \cos\lambda + \frac{V_E}{R_P+h}\right)V_E \\ \dot{\lambda} = \frac{V_N}{R_M+h}, \dot{\varphi} = \frac{V_E \sec\lambda}{R_P+h}, \dot{h} = -V_D \end{bmatrix} \quad (1)$$

As in this paper, INS is the selected as the kinematics model, it is very well known [12,13,15,19] that INS error model and the extended Kalman filter are the standard models applied to aided/INS integrated navigation systems [3]. Thus, as one can observe, from Eq.1 and considering attitude differential equations such as described in [1,13], we use a discrete time model, with quaternion based attitude instead of the Euler angles matrix, which offers the advantage to avoid singularity faced when using Euler angles [4,6,10], especially for spcecraft. The discrete-time navigation equations are then summarized such as in [3,6,10,11,12], they are given in Eq.2 to Eq.7:

$$q_{k+1} = q_k + \frac{1}{2}\left[2\left(\cos\frac{\|\omega\|}{2} - 1\right)I + \frac{2}{\|\omega\|}\sin\frac{\|\omega\|}{2}S(\|\omega\|)\right]q_k \quad (2)$$

$$\Delta v^l = R_b^l f^b \Delta t - \left(2\Omega_{ie}^l + \Omega_{el}^l\right)V^l \Delta t + g^l \Delta t \quad (3)$$

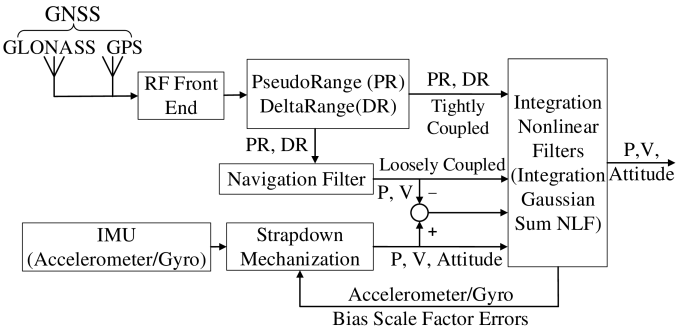

Fig. 2. Standard Aided/INS integrated navigation architecture using GPS,GLONASS

$$v_{k+1}^l = v_k^l + \frac{1}{2}\left(\Delta v_k^l + \Delta v_{k+1}^l\right) \quad (4)$$

$$\varphi_{k+1} = \varphi_k + \frac{1}{2}\frac{[v_{n,k} + v_{n,k+1}]}{R_N + h}\Delta t \quad (5)$$

$$\lambda_{k+1} = \lambda_k + \frac{1}{2}\frac{(v_{e,k} + v_{e,k+1})}{(R_N + h)\cos\varphi}\Delta t \quad (6)$$

$$h_{k+1} = h_k + \frac{1}{2}\left(v_{d,k} + v_{d,k+1}\right)\Delta t \quad (7)$$

Based on Fig.2, it is possible to reproduce similar aided navigation systems using CNS measures (attitude angles) and Pulsars X-Ray measurement of multiple epoch TOA data. It is then possible to construct differential attitude measures as a first stage in the integration Kalman filter or Gaussian Sum filter depending on the nature of noises distributions.

3. ORBIT DYNAMIC MODEL AND MEASUREMENTS

3.1 Orbit dynamic model

The analysis of orbit dynamic model for autonomous spcaceraft explorer requires that the Sun-centred inertial Cartesian coordinate system (J2000.0) is selected. The orbit dynamic model for the spacecraft is then given as:

$$\left\{\frac{dx}{dt} = v_x + w_x \frac{dy}{dt} = v_y + w_y \frac{dz}{dt} = v_z + w_z\right. \quad (8)$$

$$\begin{cases} \frac{dv_x}{dt} = -\mu\frac{x}{r^3}\left[1 - J_2\left(\frac{R_e}{r}\right)^2\left(7.5\frac{z^2}{r^2} - 1.5\right)\right] + \Delta F_x + w_{vx} \\ \frac{dv_y}{dt} = -\mu\frac{y}{r^3}\left[1 - J_2\left(\frac{R_e}{r}\right)^2\left(7.5\frac{z^2}{r^2} - 1.5\right)\right] + \Delta F_y + w_{vy} \\ \frac{dv_z}{dt} = -\mu\frac{z}{r^3}\left[1 - J_2\left(\frac{R_e}{r}\right)^2\left(7.5\frac{z^2}{r^2} - 4.5\right)\right] + \Delta F_z + w_{vz} \end{cases} \quad (9)$$

Eqs.(8) and (9) can be written in the general state equation as:

$$\dot{x}(t) = f(x,t) + w(t) \quad (10)$$

where CNS state vector $x = [xyzvNvEvD]'$. Where, x; y; z, vx; vy; vz are satellite positions and velocities of three axes respectively. r = [x y z]T is the position vector of satellite with respect to the earth. Fx;Fy;Dz are the perturbation forces which result in the high-order terms of the non-spherical perturbations in the earth's shape,

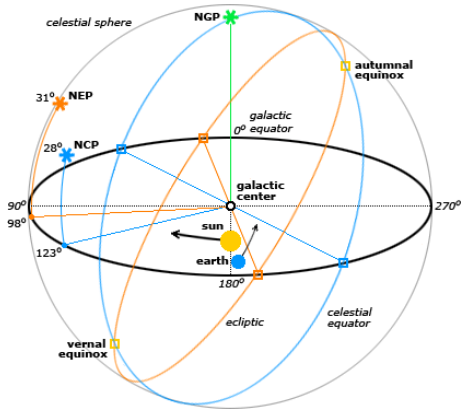

Fig. 3. Celestial sphere navigation states and parameters

the perturbation effect of the sun, moon and the sunshine pressure and the atmospheric perturbation. Re is the radius of Earth. $_{mu}$ is the gravitational constant of Earth. J2 is the second zonal coefficient. Finally, in eq.10, w(t) is the process noise with covariance Q.

3.2 Celestial Navigation Measurement

In the celestial navigation approach, Star sensors and Horizon sensors are used commonly to directly measure horizon and star direction (Direction of Arrival in case of Pulsar X-Ray signal), respectively. Because the accuracy of the star sensors measurement is typically lower than that of the elevation angle to star such as described in [1,8-11], elevation angle to star is then selected and proposed as the primary measurement source, which is defined with the other parameters related to Pulsars signal incidence in Fig.4. The elevation angle is measured between the vector n_i and the tangent to the earth surface. The measurement model is given as in [1,5-12] by:

$$\gamma = \arccos\left(-\frac{r \cdot n_i}{r}\right) - \arcsin\left(\frac{R_e}{r}\right) \tag{11}$$

where n_i is the direction vector of the X-Ray Pulsar (Crab pulsar in our case). Then, the measurement equation can be written as the following:

$$z_1(x,t) = h_1[x(t),t] + v_1(t) = \gamma + v_\gamma \tag{12}$$

where v_1 is the zero-mean white noise with variance R_{v_1}. The sensors required by the method are of small size, light weight, low power, and the corresponding measurement sampling period is of few seconds (10-100s). Even, those sensors have been widely used on-board satellites, these measures sources have demonstrated limited navigation performances with dependant parameters positioning accuracy of the order between hundreds of meters to few kilometers [1,8,9,11,12,14].

3.3 Pulsar Navigation Measurement

A pulsar timing and navigation measurement is the processing of the pulse TOA observed by X-ray sensor at the spacecraft and predicted by pulse timing model at the *ssb* [5-14], see Fig.4. As described in the literature, The pulse TOA measured at the spacecraft location, called t_{sc}, can be transferred to its corresponding time at the *ssb*, t_{ssb}. In eq.13, one can observe the relation and the timing transformation from the spacecraft TOA into the solar system barycenter TOA.

$$\begin{aligned} t_{ssb} = \\ t_{sc} + \frac{1}{c} n \cdot r_{sc} + \frac{1}{2cD_{ps}} \left[-r_{sc}^2 + (n \cdot r_{sc})^2 \right. \\ \left. -2b \cdot r_{sc})^2 - 2b \cdot r_{sc} + 2(n \cdot b)(n \cdot r_{sc})\right] \\ + \frac{2\mu_{Sun}}{c^3} \ln \left| \frac{n \cdot r_{sc} + r_{sc}}{n \cdot b + b} + 1 \right| \end{aligned} \tag{13}$$

where c is the speed of light. D_{ps} is the range from pulsar to *ssb*. b is the position vector of the *ssb* relative to the Sun. Sum is the gravitational constant of the sun. n is the direction vector of the pulsar. r_{sc} is the position vector of the satellite with respect to the*ssb*, r_e is the position vector of Earth with respect to the *ssb*, r is the position vector of the satellite with respect to Earth, and can be transferred to r_{sc},one can write the second measurement equation by assuming zero bias clock model, which can be justified by the time difference of arrival, eliminating bias naturally, by the following equation:

$$z_2 = h_2[x(t),t] + v_2(t) = t_b - t_{sc} + v_t \tag{14}$$

where vt can be presented as:

$$p(v_t) = (1-\epsilon)N(0,\sigma_1^2) + \epsilon N(m_2,\sigma_2^2). \tag{15}$$

In this paper, we consider a short observation time period of pulsar X-ray signals, which is assumed to be disturbed by non Gaussian distributions instead of white Gaussian noises. In addition, colored noises were already encountered in previous analysis by the use of H_{inf} filtering approaches. Even if this technique has been tested in simulation, it doesn't appear in this work and will be discussed in future survey paper prepared by the authors.

It is important to mention that the experimental and empirical statistical measurement variance when noises are considered Gaussian can be calculated or estimated such as demonstrated in [1,2,5,7-13]. In our case, Pulsar noises are considered non-Gaussian and requires other estimation algorithms.

3.4 Brief note on Pulsars GDOP

The geometric dilution of precision (GDOP) is an expression of the accuracy of the estimated three-dimensional position. Scuh as well defined for GPS positioning related problems, GDOP is based on the covariance matrix

Table 1. **of Crab pulsar (PSR B0531+21) parameters**

Parameter	Value
Right ascension (J2000)	5 h 34 min 31.972 s
Declination (J 2000)	5 h 34 min 31.972 s
Galactic longitude	184.5575°
Galactic latitude	−5.7843°
Frequency, Hz	0.0335040932
Period, s	0.0335045369458
Frequency derivative, Hz/s	4.205296×10^{-13}
Period derivative, s/s	$4.2052296 \times 10^{-13}$
Epoch of ephemeris, MJD	51527.0000001373958

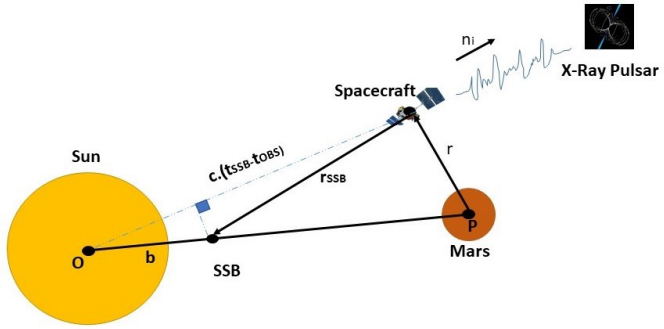

Fig. 4. Pulsar Based Positioning and Timing SoOP for Mars orbital satellite

of the estimated errors of the position. The difference resides in the ranging and timing measurement sources, which in this paper are X-ray pulsars. If one consider optimal exploration probe trajectory related to a pulsars network in the universe, It will be possible using fisher information matrix to determine the optimal set of chosen pulsars that will compute the best universal positioning solution. Such as explained by the authors in [5;6], If pulsars are selected from limited view of the celestial sky, the measurement matrix will then inadequately skew the observations toward this direction and will not perform the best three-dimensional solution. At the opposite, If pulsars are well distributed in the celestial sky, thus, better three-dimensional solution can be achieved. like in GPS positioning framework, Lower values of GDOP indicate better distribution. Finally, each pulsar is related to the exploration spacecraft position by two fundamental measures: range , or phase , defined and extracted from the signals received through the LOS (line of Sight) direction from the pulsars. GDOP equations are given below in as:

$$GDOP_{\text{ps}} = \sqrt{\text{tr}\,(G')} = \sqrt{\sigma_x^2 + \sigma_y^2 + \sigma_z^2 + \sigma_t^2} \qquad (16)$$

The position dilution of precision (PDOP) can be determined from this system by considering only the position related states as

$$\text{PDOP}_{\text{ps}} = \sqrt{\text{tr}\left(G'_{3\times 3}\right)} = \sqrt{\sigma_x^2 + \sigma_y^2 + \sigma_z^2} \qquad (17)$$

The time dilution of precision (TDOP) is directly computed by the time variance in this matrix as:

$$TDOP_{ps} = \sigma_t \qquad (18)$$

For further details on the GDOP estimation and demonstration of Pulsars measurement matrix, readers can refer to [12].

4. HIGH DEGREE H INFINITY INFORMATION FUSION ALGORITHM

Because CNS and Pulsar X-ray measurement are a combination of two Gaussian distributions, White and colored, the architecture and the designed filters proposed in this paper define a new framework solution by using Gaussian sum filtering approach with two different Gaussian distribution densities. To achieve good performances, multiple quadrature Kalman filters based on different quadrature rules and nonlinear transformations are developed in this work.

In [12], authors proposed to develop two-level filter to fuse the navigation data between CNS and Pulsars. They proposed to use in cascade UKF with H infinity filter in order to handle non-linearity of CNS measures, and colored noises affecting the Pulsar measurement. In this work, however, extended data fusion between INS, CNS and pulsar navigation was adopted based on Gaussian sum multiple Quadartaure Kalman filtering approaches. Ongoing work is devoted to develop a non-Gaussian sum filtering [17], a new framework as a generalized robust filtering solution to the problem of Deep Space multi Sources Information fusion is then under development.

Non-Gaussian noises The Observation matrix is composed by two measurement data-set, CNS and X-Ray pulsars (range and/or Phase) signals, both are considered as a strongly nonlinear[17,18,19]. The non-Gaussian noise simulated in this paper is defined in Eq22 and Eq23 given below:

$$f(x) = \frac{1-\epsilon}{\sqrt{2\pi\sigma_1^2}} \exp\left(-\frac{x^2}{2\sigma_1^2}\right) + \frac{\epsilon}{\sqrt{2\pi\sigma_2^2}} \exp\left(-\frac{(x-m_2)^2}{2\sigma_2^2}\right) \qquad (19)$$

A. Gaussian Mixture Noise model

$$p(n(k)) = (1-\epsilon)N(0,\sigma_1^2) + \epsilon N(m_2,\sigma_2^2). \qquad (20)$$

where σ_1^2 is the 1st Gaussian density variance, σ_2^2 the 2nd Gaussian density variance, and ϵ contamination coefficient.

In this paper, a Gaussian sum filter such as described in [19-13] may be used to propagate and update the conditional PDF. Since all the components of the mixture PDF are Gaussian and thus, only estimates of their mean and covariance need to be propagated between t_k and t_{k+1} using the proposed multiple degree Cubature Kalman filter 3rd deg CKF time update equations:

$$p(t_0, x_0) = \sum_{i=1}^{N} \omega_0^i N(x_0|\mu_0^i, P_0^i), \qquad (21)$$

where $N(x|\mu,P) = |2\pi P|^{-1/2} \exp\left[-\frac{1}{2}(x-\mu)^T P^{-1}(x-\mu)\right]$ and $\sum_{i=1}^{N} \omega_{t|k}^i = 1, \omega_{t|k}^i \geq 0, \forall t$.

4.1 High-degree Cubature Information Filters

Cubature Kalman filters were developed by authors in [35]. These filters came outperform the previous Sigma Point Kalman Filters SPKFs developed by famous specialists in [35,36]. The major achievement was the development of the Unscented filter based on the unscented transform [36] which was presented as a revolutionary nonlinear approximate Kalman filter, which provided much better performances than the traditional but powerful Extended Kalman Filter (EKF). The nonlinear filtering problem statement remains the same and is given by the following equations:

$$\begin{aligned} x_k &= f(x_{k-1}) + v_{k-1}, \\ z_{k,m} &= h_m(x_k) + n_{k,m}, \end{aligned} \qquad (22)$$

where m stands for number of Pulsars source of timing (TOA) measures, or what we can consider as a scpace

based SoOP (Signals of Opportunity). For simplicity, in this paper, we consider only one source of SoOP, however, in the future, we can consider an heterogeneous sensors network by considering simultaneous different X-Ray Pulsars from different galaxies.

Based on the simulation and analysis, and due to the high degree of non linearity, we propose to develop Multi Quadrature Kalman filters with different degrees. Different algorithms of numerical computation are described in the following sections. The quadrature rules are numerical methods to approximate the Gauss integral [7-11]. Algorithm-1 describe a generalized Quadrature Kalman Filter proposed by authors in [10], in which depending on the weight and points calculations, can be equivalent to UKF,CKF, HCKF and GHKF [11].

5. SIMULATION RESULTS

In this section, we have developed simulations based on INS/CNS/Pulsars data fusion for deep space navigation under two parallel scenarios: (1) Gauss Quadrature Kalman filters under non-Gaussian measurement noises (CNS and Pulsars) (2) Gaussian Sum Quadrature Filters under non-Gaussian noises affecting the combined (CNS/pulsar measurement). From Fig.5 to Fig.8, one can observe the improvement caused by the transformation into the Gaussian Sum framework based on different quadrature, on Velocity and Attitude estimation problems. Simple case was assumed in which the Spacecraft doesn't operate any rotation and has transitional velocity vector. In summary, The simulation condition is as follows:(1) The elements of Spacecraft orbit: semi-major axis: a = 7136:635km, eccentricity:$e = 1.809 \times 10^{-3}$, inclination $i = 65°$, right Ascension of the ascending node: $\omega = 30°$ the argument of perigee: $\Omega = 30°$. (2) The accuracy of the devices:the accuracy of star sensor: $3''(1\sigma)$. the accuracy of horizon sensor: $0 : 02(1\sigma)$. the area of X-ray sensor: 1m^2. (3) Navigation star the stellar database: the Crab pulsar. (4) The sampling period pulsar navigation subsystem: 1s. For celestial navigation subsystem period is set at: 1s. Thus, for the process co variance, large values are considered such as in: $Q = \text{diag}\left[(100\text{m})^2, (100\text{m}^2, (100\text{m}^2, (1\text{m/s})^2 \ \ (1\text{m/s})^2, (1\text{m/s})^2\right]$. Finally, all nonlinear filters : quadrature Kalman and Gaussian Sum based were initialized using the same parameters values.

6. VI. CONCLUSION

After analysis of different estimation results based on QKF algorithms and GS-QKF algorithms for different Spacecraft navigation states, it appears that CNS/Pulsar measurement information fusion with INS represent a good solution for deep space autonomous navigation. Indeed, QKFs, can perform well when processing CNS and Pulsars X-Ray measurement individually, however for dual and parallel processing, the proposed Gaussian Sum filters outperform clearly the standard navigation filters. The limitations of previous methods based on H_{inf} methods were expanded to new positioning and navigation performances. At the end, as a perspective for next steps of this research, a new hybrid framework between H_{inf} and GS could be considered in the next upcoming publication.

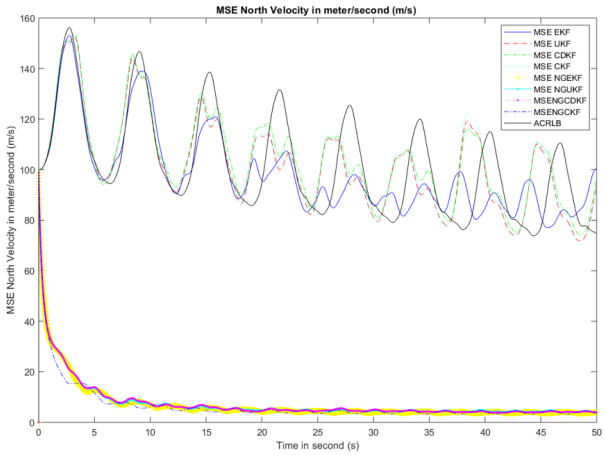

Fig. 5. North velocity estimation error with QKFs and GS-QKFs

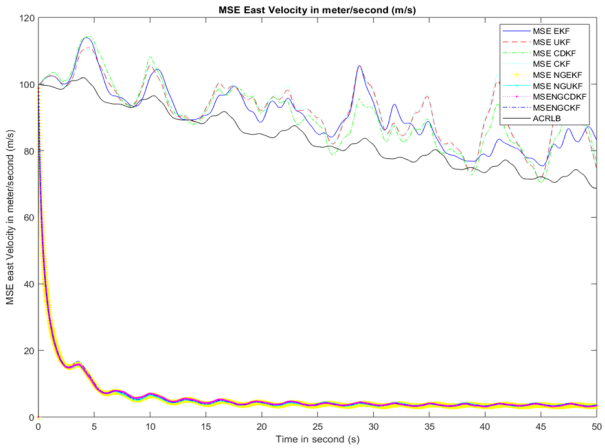

Fig. 6. East velocity estimation error with QKFs and GS-QKFs

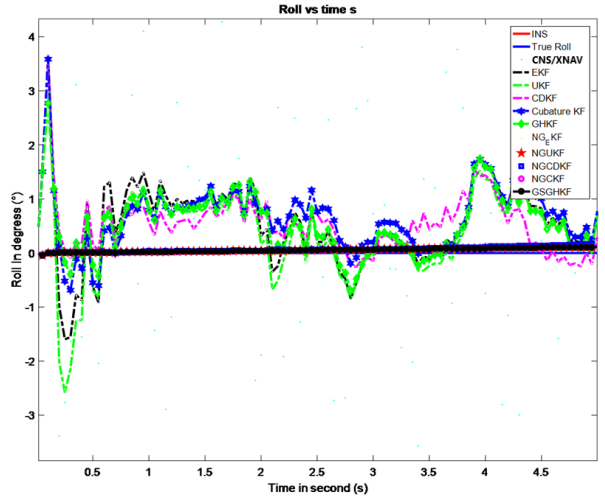

Fig. 7. Roll Attitude estimation error with QKFs and GS-QKFs

Algorithm 1. Gauss Quadrature Kalman Filters
Input :x_{k-1},P_{k-1},u_k,z_k **Output** :x_k^-,P_k^- **return**x_k^-,P_k^-
Assume at time k that the posterior density function is known. Cholesky factorization can be given as follows:

$$P_{k-1/k-1} = \sqrt{P_{k-1/k-1}}(\sqrt{P_{k-1/k-1}})^T. \tag{23}$$

The quadrature points $\{X_{l,k-1/k-1}\}_{l=1}^m$ are given in Equation (6). The matrix square root is the lower triangular Cholesky factor provided in Equation (7). The estimate of the predicted state mean and the estimate of the predicted error covariance are given in Equations (8) and (9), respectively.

$$X_{l,k-1/k-1} = \sqrt{P_{k-1/k-1}}\xi_l + \hat{x}_{k-1/k-1} \tag{24}$$

$$\chi^*_{l,k/k-1} = f(X_{l,k-1/k-1}, u_{k-1}, k-1) \tag{25}$$

$$\hat{x}_{k/k-1} = \sum_{l=1}^{m} \omega_l \chi^*_{l,k/k-1} \tag{26}$$

$$P^-_{x_k} = \sum_{l=1}^{m} \omega_l \chi^*_{l,k/k-1}\chi^T_{l,k/k-1} - \hat{x}_{k/k-1}\hat{x}^T_{k/k-1} + Q_{k-1} \tag{27}$$

The Cholesky factorization $P_{k/k-1}$, the quadrature points $X_{l,k/k-1}$, the predicted measurement $Y_{l,k/k-1}$, the average prediction $\hat{y}^-_{k/k-1}$, the innovation covariance matrix $S_{k/k-1}$, the cross-covariance matrix $P_{xy,k/k-1}$, the quadrature Kalman gain W_k, the state $\hat{x}_k$, and the error covariance $P_{k/k}$ are updated as follows:

$$P_{k/k-1} = \sqrt{P_{k/k-1}}(\sqrt{P_{k/k-1}})^T, \tag{28}$$

$$X_{l,k/k-1} = \sqrt{P_{k/k-1}}\xi_l + \hat{x}_{k/k-1}, \tag{29}$$

$$Y_{l,k/k-1} = h(X_{l,k/k-1}), \tag{30}$$

$$\hat{y}^-_{k/k-1} = \sum_{l=1}^{m} \omega_l Y_{l,k/k-1}, \tag{31}$$

$$S_{k/k-1} = \sum_{l=1}^{m} \omega_l Y_{l,k/k-1}Y^T_{l,k/k-1} - \hat{y}_{k/k-1}\hat{y}^T_{k/k-1} + R_k, \tag{32}$$

$$P_{xy,k/k-1} = \sum_{l=1}^{m} \omega_l X_{l,k/k-1}Y^T_{l,k/k-1} - \hat{x}_{k/k-1}\hat{y}^T_{k/k-1}, \tag{33}$$

$$W_k = P_{xy,k/k-1}S^{-1}_{k/k-1}, \tag{34}$$

$$\hat{x}_k = \hat{x}_{k/k-1} + W_k(y_k - \hat{y}_{k/k-1}), \tag{35}$$

$$P_{k/k} = P_{k/k-1} - W_k S_{k/k-1} W^T_k. \tag{36}$$

The Gauss Quadrature Kalman Filter algorithm describe above is a generalized form of Gauss-Hermite, Cubature, Unscented as well as other recently developed nonlinear filters such as Gauss Chebychev, Gauss Laguerre,etc. The difference between all these algorithms is how quadrature points and weights are constructed.

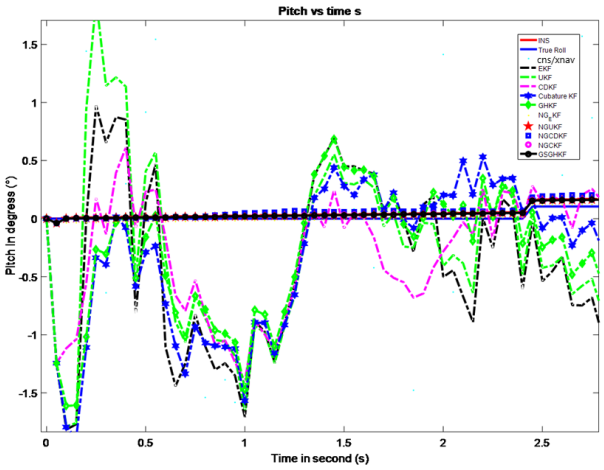

Fig. 8. Pitch Attitude estimation error with QKFs and GS-QKFs

REFERENCES

[1] Wang, Y., Zheng, W., An, X., Sun, S., Li, L. (2013). XNAV/CNS Integrated Navigation Based on Improved Kinematic and Static Filter. Journal of Navigation, 66(6), 899-918.

[2] LIU Jin, MA Jie and TIAN Jinwen, CNS/Pulsar Integrated Navigation Using Two-level Filter, Chinese Journal of Electronics -Vol.19, No.2, Apr. 2010.

[3] J. Morales, J. Khalife, A. Abdallah, C. Ardito, and Z. Kassas ,Inertial navigation system aiding with Orbcomm LEO satellite Doppler measurements. ION Global Navigation Satellite Systems Conference, Sep. 24-28, 2018, Miami, FL.

[4] Benzerrouk, H.; Nebylov, A.; Li, M. Multi-UAV Doppler Information Fusion for Position Determination Based on Distributed High Degrees Information Filters. *Aerospace***2018**, *5*, 28.

[5] R. Lopez, J. Malardé, F. Royer and P. Gaspar, "Improving Argos Doppler Location Using Multiple-Model Kalman Filtering," in *IEEE Transactions on Geoscience and Remote Sensing*, vol.52, no.8, pp.4744-4755,Aug.2014.

[6] Hao Liang and Yafeng Zhan, "A Fast Detection Algorithm for the X-Ray Pulsar Signal," Mathematical Problems in Engineering, vol. 2017, Article ID 9607821, 5 pages, 2017.

[7] Chester, T.J., Butman, S.A., 1981. Navigation using X-ray pulsars. In: NASA Technique Report 81N27129, pp. 22–25.

[8] Downs, G.S., 1974. Interplanetary navigation using pulsating radio sources. In: NASA Technique Report 74N34150, pp. 1–10.

[9] Liebe, C.C., 2002. Accuracy performance of star trackers - a tutorial. IEEE Trans. Aero.Electron. Syst. 38 (2), 587–599.

[10] Liebe, C.C., Murphy, N., Dorsky, L., Udomkesmalee, N., 2016. Three-axis sun sensor for attitude determination. IEEE Aero. Electron. Syst. Mag. 31 (6), 6–11.

[11] Jiandong Liu, Shuanggen Jin, Evaluation of Mars probe positioning using X-ray pulsars, celestial, gravity-aided and ground-based measurements, Planetary and Space Science, Volume 163, 2018, Pages 14-34, ISSN 0032-0633.

[12] Shuanggen Jin, Jörn Helbert, New advances in interdisciplinary observation and understanding of the solar system, Planetary and Space Science,Volume 163,2018,Pages 1-4, ISSN 0032-0633.

[13] Anderson, K.D., Pines, D.J., Sheikh, S.I., 2015. Validation of pulsar phase tracking for spacecraft navigation. J. Guid. Contr. Dynam. 38 (10), 1–13.

[14] Becker, W., Bernhardt, M.G., Jessner, A., 2013. Autonomous spacecraft navigation with pulsars. Acta Futura 7, 11–28.